Observation of the redistribution of nanoscale water filled porosity in cement based materials during wetting.

N Fischer, R. Haerdtl, P. J. McDonald

HeidelbergCement Cement Technology Center, Leimen, Germany

Micro and NanoMaterials and Technologies Industrial Doctorate Centre

Department of Physics, University of Surrey, Guildford, Surrey, GU2 7XH

Abstract

This paper presents investigations which have been made through spatially resolved ^{1}H NMR T_2 relaxation time analyses of Portland cement mortars and concretes. Experimental data show that the initial ingress of water into previously dried cement based materials is accompanied by a subsequent re-arrangement of that water within the nano-scale porosity in which it resides. Such an observation is surprising but lends support to earlier observations of a sharp decrease in the absorption rate of water into dried cement based materials {{4 Hall,C. 1995;}}. It also lends support to the idea of C-S-H shrinkage followed by swelling when water egresses and subsequently reinvades cement based materials {{73 Taylor,S.C. 1999;}}.

Introduction

[RHa1]. The NMR signal intensity is directly proportional to the amount of ^{1}H and hence water in the sample. T_2 is the NMR signal lifetime. For water in the pore spaces, it is well known that T_2 correlates linearly with the pore volume to surface ratio, that is the pore size. and hence that the T_2 distribution reflects the water filled pore size distribution {{91 Valori,A. 2013;}}. In the case of never-dried, hydrated white Portland cement measured at ^{1}H frequency of 7.5 MHz, separate T_2 components (from long to short) are normally seen representing

water in capillary pores (> 0.1 μm, >10 ms), inter-hydrate spaces (circa 10-50 nm, 1-5 ms), hydrate gel pores (2-5 nm, 200-500 μs) and hydrate inter-layer spaces (~1 nm, ~100 μs) {{82 Muller,Arnaud C.A. 2013;}}. These times are generally lower in grey cement due to additional paramagnetic impurity relaxation. A further very short T_2 component for water in crystalline phases can also be seen in appropriate experiments. Muller et al measured the desorption isotherm of white Portland cement using the same method and showed that as the sample is equilibrated at ever lower relative humidity, so water is lost successively from larger pores down to small pores {{83 Muller,A.C.A. 2013;}}. Gajewicz continued this by measurement of the subsequent absorption branch of the isotherm and also a secondary desorption branch (Agata PhD thesis[N2]). hysteresis was observed, mainly originating in the gel porosity. Zamani et al {{84 Zamani,S. 2014;}} measured the spatial profile of the T_2 distribution in a cement paste exposed to and equilibrated under an RH gradient for more than 1 year and from this calculated the water relative permeability during primary desorption.

The observations made in this work go beyond these earlier studies in that they examine the T_2 distribution as a function of spatial position within the sample *during* rewetting after first drying rather than for the equilibrated sample. The results vary slightly from one cementitious material to the next, but the underlying features are the same. Water initially invades the dried material. A concentration close to full saturation, if not full saturation, is rapidly achieved in the surface layers. As water continues to penetrate to deeper layers, the T_2 distribution within the surface layers changes so as to decrease the longest T_2 components representing the interhydrate /capillary porosity.

Experiments were performed using two different NMR systems. The first is a portable Surface GARField operating at ^{1}H frequency 2.8 MHz {{85 Aptaker,P.S. 2007; 48 McDonald,P.J. 2007;}}. This instrument is designed to profile into the surface of large samples and flat structures. It readily records signal to a depth of a few centimetres with millimetre resolution. It samples a large surface area of circa 225 cm^2 (i.e. 150 mm × 150 mm). Samples used with this system are typically large blocks of concrete. The second system is a

laboratory GARField {{86 Glover,P.M. 1999;}} operating at ^{1}H frequency 23.4MHz. This instrument can profile long cylindrical samples of diameter 18 mm with a spatial resolution of a few microns, although in this study a much coarser resolution, 1 mm, was used. Samples were mortars and concretes cured both sealed and underwater for up to 6 months.

The new data should contribute to answering a number of evolving questions concerning pore-water interactions in cement based materials. As well as the observations of a dramatic slowdown in the rate of absorption during sorption tests and the question of C-S-H swelling already mentioned, other topics of current discussion upon which the results may shed light are: what is the nature of the nanoscopic damage caused to C-S-H by drying of cement and is it reversible {{19 Collier,N.C. 2008;}}; does the relative water permeability of cement show hysteresis with respect to the degree of water saturation above and beyond the well known hysteresis with respect to relative humidity [Zhidong Zhang?[N3]]; and does the depth of water penetration by NMR to other more traditional indicators? The last question in particular will be addressed in future publication based on some of the current results.

Materials and Methods

Materials

Concrete was designed with 0.5 water-to-cement (w/c) ratio by mass and 30 volume % paste by volume and 1.5 volume % air content using Portland cement. The aggregate fractions used were 0/2 mm sand (30 volume %) and 2/8 mm gravel (38 volume %). Standard mortar (EN 196-1) with a ratio of 0.5:1:3 by mass for water:cement:aggregate was mixed using Portland cement. Both the concrete and mortar were cast in 150 mm cubes. One day after mixing, the cubes were demoulded and either put under lime water (underwater curing) or sealed in a double layer of plastic sheet (sealed curing). Samples were cured at 20 °C for

a minimum of 3 months. A limited number of concretes with w/c = 0.8 were also made.

After curing, 150x150 mm^2 concrete slabs were wet cut from the middle of the cubes with the cut faces parallel to the casting-surface face. The slab thicknesses were variably 40, 70 and 100 mm for surface GARField analysis. In the case of the mortars, 18 mm diameter cylinders of length 150 mm were wet cored from the 150 mm cubes for laboratory GARField analysis. All cores with the same curing condition were taken from the same cube. The paste skin that forms on the surface of the sample at casting was not removed from the end of the cylinders.

Concrete slabs were oven dried at 60°C to constant mass in a standard oven. This typically required 1 month. The mortar cylinders were dried to constant mass under light vacuum to minimise carbonation at the same temperature in typically 2 weeks. At 60°C, it is expected that the capillary, interhydrate and C-S-H gel pores empty, but that the C-S-H interlayer water remains as evidenced by NMR {{50 McDonald,P.J. 2010;}}.

After drying, the sides of the samples were sealed with PTFE tape. Other common sealants and tapes, e.g. epoxy coating or parafilm® could not be used as they give a significant ^{1}H background signal in NMR. The PTFE wrapping was used to inhibit surface drying and encourage a one-dimensional water transport across the sample thickness (slabs) or length (cylinders).

Dried samples were subsequently exposed to liquid tap water on one exposed side/end. In the case of concrete slabs for the surface GARField experiments, the slabs were stood on saturated foam in a pool of water in a large plastic container. In the case of the mortar cylinders, the samples were suspended such that the lower end dipped 1-2 mm into a shallow pool of water. The water levels were maintained constant by regularly replacing absorbed and/ or evaporated water.

NMR measurements

Due to wet cutting, the pre-drying sample mass is of no real significance, especially for sealed cured material. Hence, the sample mass was measured after drying, at 1, 2, 4 and 8 hours, then 1, 2, 4, 7 and 14 days. Data at 4 days was only recorded for mortar samples. Samples were taken out from the water, the surface in contact with water was dabbed dry with a paper towel and the mass measured. For mass measurement, the samples were removed from water for a maximum of 30 s.

NMR data in the form of relaxation echo decay profiles were acquired after 1, 2, 4, 7, 14 and, in limited cases, 28 days of capillary sorption. During the measurement, the sample ends were covered in plastic film to avoid drying. As opposed to the sample sides, the sample ends do not affect the depth resolved measurements. The relaxation measurements were made using the Carl-Purcell-Meiboom-Gill (CPMG) pulse sequence {{88 Meiboom,S. 1958;}} in both NMR systems. Profiles were generated with the Surface GARField using, for the most part, 1 mm motor steps. The maximum profile length is 30 mm, the first 5 mm of which is above the sample surface, within the Perspex® facing of the instrument. Data acquisition parameters were optimised for maximum signal-to-noise ratio. Therefore the pulse length varied by depth. At each depth, 12 echoes were recorded with an echo spacing of 130 µs and 4k averages. For spot measurement of T_2 with enhanced signal-to-noise ratio 3 mm into the wet surface, data was acquired for 20 echoes with 16k averages. For the laboratory GARField at 23.4MHz, the pulse length was 6.5 µs, and the echo spacing was 64 µs. 64 echoes were recorded with 2k averages at each depth. The profile step was again 1 mm in regions of interest, near the sample ends, more elsewhere. The repetition delay was 0.25 s for both systems, taking about 8.5 minutes to record echo train dataset for the laboratory GARField and about 1 hour for the Surface GARField with enhanced signal-to-noise ratio.

The Surface GARField measurement was calibrated using a saturated sandstone of the same lateral dimensions as the concrete samples, 150 x 150 mm^2. The sandstone was uniformly wet on this scale. A sandstone profile was acquired with the same parameters as the concrete (pulse length, pulse gap and motor step) though with double the number of averages. Also more echoes

were recorded. The signal amplitude decreases with depth due to the decreasing sensitivity of the detector. The profile acquired from uniformly wet sandstone was used to compensate for this effect. Further, the sandstone that had known water filled porosity was used to calibrate the porosity measurement. Echo sum was used for the profiles to improve signal-to-noise ratio and the difference in relaxation time for sandstone and concrete was taken into account in the calibration and a correction factor was introduced. The laboratory GARfield was calibrated using both a saturated sandstone core and a rubber reference sample, the latter used to correct for pulse duration artifacts {{92 Benson,T.B. 1995;}}.

NMR analysis

Profiles were generated from echo sum data. Echo sum improve the signal to noise ratio, but at the cost of over emphasising the long T2 components in the signal. In the case of concrete, where a single exponential decay fitting was used (see below), the profiles were calibrated against the sandstone taking into account the difference in relaxation time between sandstone and concrete. Hence a rough measure of filled porosity is possible.

The first few echoes of a CPMG recorded in a strong field gradient such as GARField are subject to systematic amplitude modulation {{90 Hürlimann,M.D. 2000;}}. In case of the Surface GARField with concrete samples, the first echo was never used and the second echo was also disregarded for T_2 analysis. In the case of the laboratory GARField and mortar samples, the echo amplitudes were corrected using a rubber reference. For improved signal to noise ratio, the average of 11 slices was used for exponential fitting. GARField data is generally of lower signal to noise ratio than that acquired for bulk samples using homogeneous magnets. Therefore inverse Laplace transformation cannot be used to discover the T_2 distribution. In the case of concrete samples measured using the surface GARField, the data was fit to a single exponential decay plus a baseline representing Interhydrate and capillary pore water. The first two echoes that are affected by pulse artefact and that contain a contribution from gel pore water were disregarded. In this case of mortar samples, the data was fitted with 2 components at fixed relaxation times, 250 μs and 1250 μs plus a

baseline. Pulse artefacts were eliminated by reference to the rubber sample. A further discussion of these choices is found in section ??? These values were chosen based on prior experience and literature reports and on multiple different fitting analyses. The 250 μs component is characteristic of gel porosity in Portland (grey) cement; that at 1250 μs of interhydrate water. The baseline represents a small contribution from long components due to water in large capillaries. Shorter components due to, e.g. hydrate interlayer water are not seen from Portland cement in GARField (although they are seen in white cement).

Results and analysis

Concrete samples

The top left element of Figure 1 shows the profile through the surface 15 mm of one face of a concrete cube of side length 150 mm cured underwater for 3 months before drying. The first 5 mm of the profile is recorded above the sample within the magnet Perspex® facing. The profile was acquired with 2 mm steps using the surface GARField magnet and a CPMG echo train as described in the methods section. The profile shown represents the sum of echoes 2-10. The first echo is disregarded since it is subject to considerable experimental artefact. Echoes beyond the 10^{th} are disregarded because the signal to noise ratio decreases below unity. The profile intensity is normalised to that for uniformly saturated sandstone.

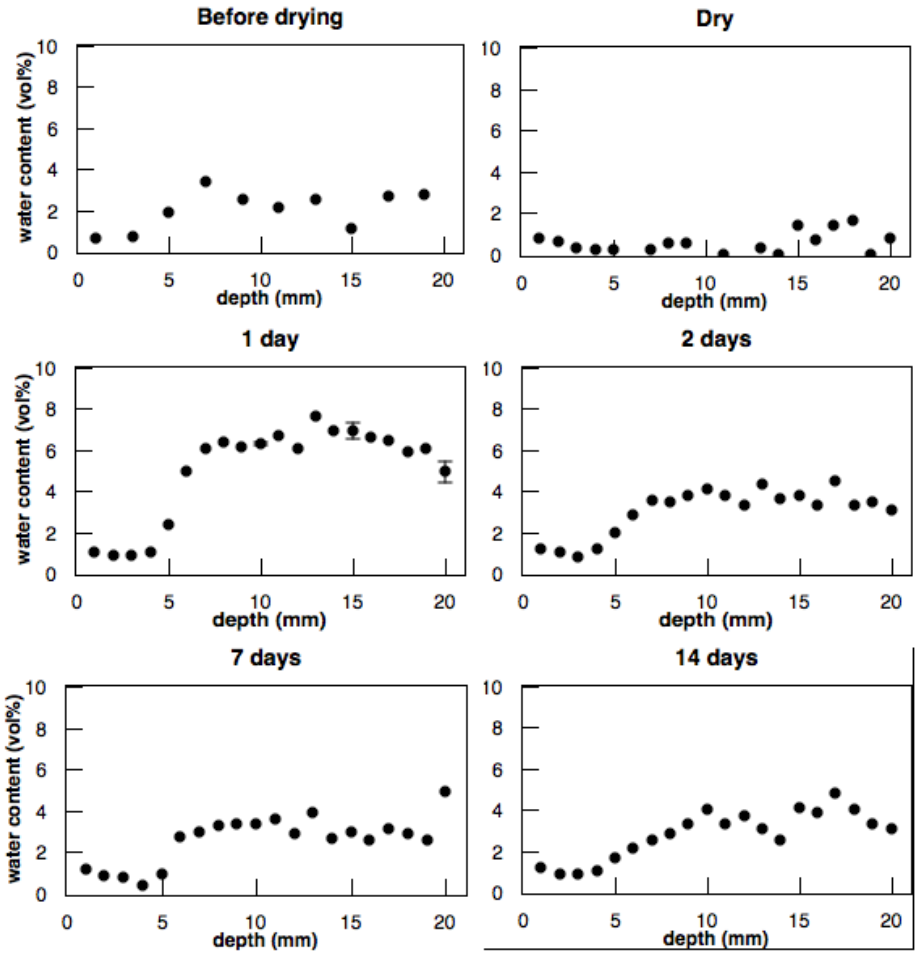

209

210 Fig. 1 echo sum profiles of underwater cured concrete before and after
211 drying and at different times of capillary sorption. The sample surface is at 5 mm
212 along the depth axis.

213

214 The top right element of Figure 1 shows the profile into the top 15 mm of
215 a block dried at 60 °C for 4 weeks. The profile was acquired with 1 mm steps. No
216 significant signal is observed.

217 The block face is now exposed to liquid water in a capillary uptake
218 experiment and the resultant profiles at different absorption times are shown in
219 the subsequent figure elements. Specifically, the profile is shown after 1, 2, 7 and
220 14 days. Three observations can be made. The first is that water penetrates into
221 the top 15 mm in 1 day. In fact, measurements from both sides of other slabs not
222 shown suggest that water typically penetrates fully across 40 mm thick slabs in
223 1 day, but not 70 mm slabs. The second observation is that the echo sum

intensity is greater after 1 day of capillary absorption than it is in the never-dried, underwater-cured sample. The third observation is that after the first day of capillary absorption, the echo sum intensity decreases back down towards the initial values across the top 15 mm.

The 1 day data gives an estimate of the measurement errors. The error bars shown here are errors in the mean derived from 5 repeats of the measurement at 10, 15 and 20 mm depth. Notice that the absolute error increases with depth, due to the decreased instrument sensitivity. Moreover, the essential trend of a maximum in the echo sum data after about 1 day of capillary absorption has been observed in all of the 20[N4] samples studied.

All further concrete sample results shown are higher signal to noise ratio spot measurements of relaxation times taken from 3 mm below the surface of cut faces. The results span 7 samples: 2 sealed cured, 0.5 w/c ratio concretes, 3 sealed cured 0.8 w/c ratio concretes and 2 underwater cured 0.5 w/c ratio concretes. They all show essentially the same results, but are displayed in these separate groupings.

Figure 2 is the T_2 echo decay for a 0.8 w/c sealed cured concrete recorded before drying, and after 1, 2, 7, 14 and 28 days exposure to water. Echoes 3-20 were fit to a single T_2 decay representing the capillary and interhydrate water in the sample. The first echo was disregarded due to artefact, the second as it contains a significant element of gel-pore water. The standard error in the mean of the fitting of one sample (measured on a sealed cured 0.5 w/c sample) measured 5 times was about 1.2 % for the intensity and about 2.5% for the T_2 relaxation time. Across three different samples made from the same original mix, the standard error for both intensity and T_2 was about 2%. The standard error was calculated for all groupings and and gave similar results. Hence we estimate a total error of circa 3% for intensity and 5% for T_2.

[RHa5]

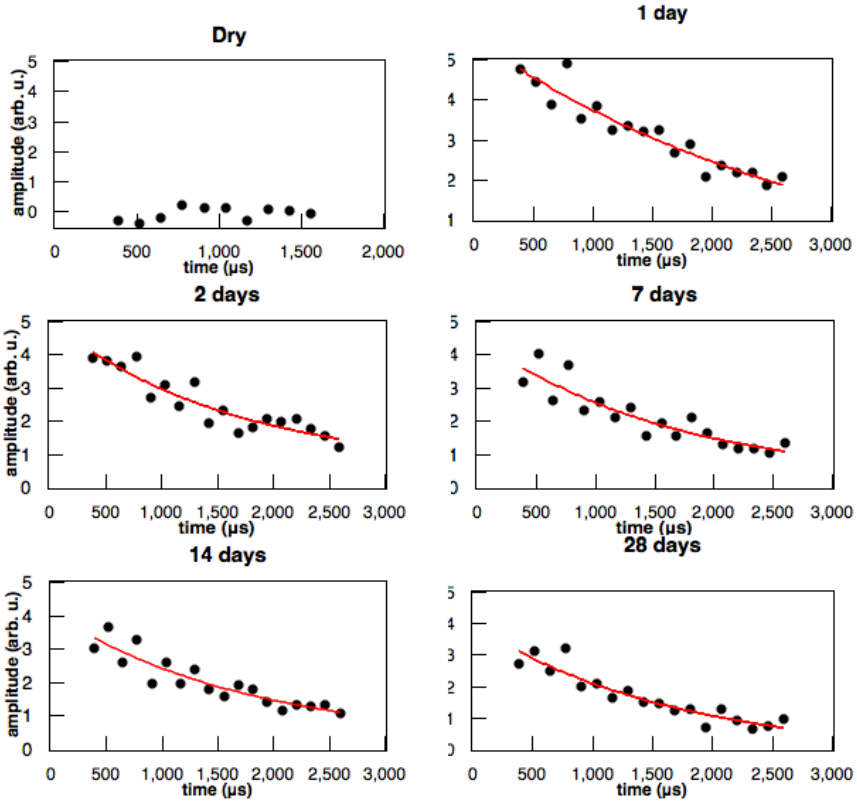

Fig 2. Echo decay data and associated single component exponential plus base line fits of sealed cured 0.8 w/c ratio concrete measured 3 mm from the wet surface at different times of capillary sorption.

The fitting analysis results are shown in Figure 3 for all three sample groupings. In every case, during re-wetting, the surface capillary water signal decreases. In case of underwater cured, the decrease is to the as-cured value. The T_2 likewise increases above the as cured value before decreasing. Error was based on multiple samples of the same group and the relative changes to 1 day signal amplitude.

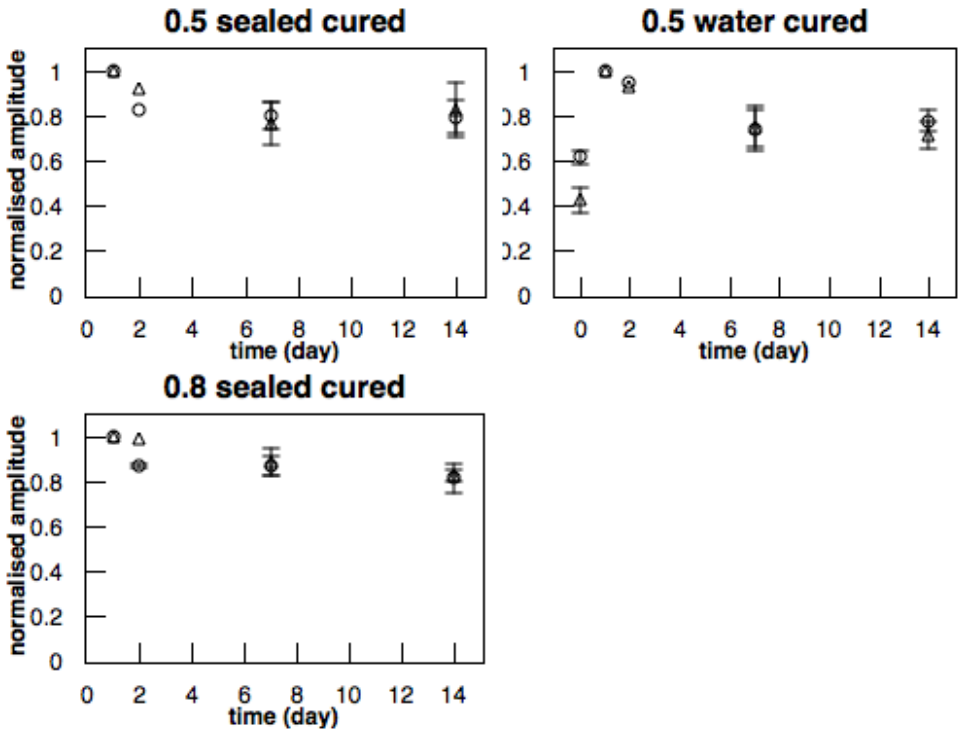

264

265 Fig 3. Normalised signal intensity (triangles) and T_2 (circles) at 3 mm
266 depth as a function of capillary absorption time. In the case of under water cured
267 samples, the data at 0 days is for the never dried concrete.

268

269 Fig 4. shows the water uptake by gravimetry for w/c = 0.5 sealed cured
270 concretes with 40, 70 and 100 mm thickness. Water uptake slows down
271 significantly after 1 day of sorption in all sample sizes. Water uptake obviously
272 slows down when the waterfront reaches the top of the sample, as it was the
273 case for the 40 mm thick sample. However, the 70 and 100 mm thick samples
274 were measured at the top by NMR and showed no signal after 1 day.

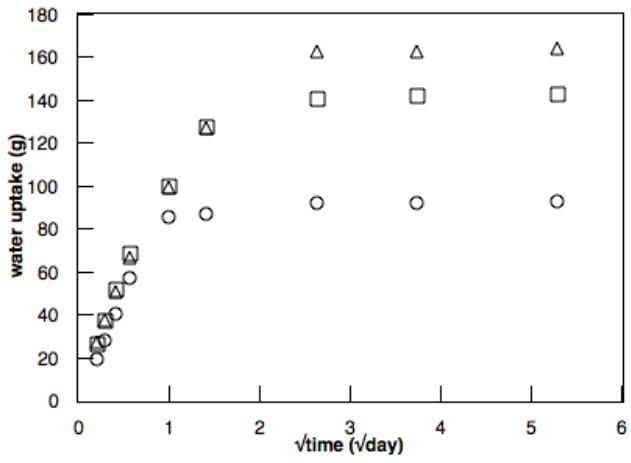

275

Fig 4. Gravimetric water uptake of 0.5 *w/c* sealed cure concretes for 40 (circle), 70 (square) and 100 mm (triangle) thick slabs.

Mortar samples

In order to better quantify all the evaporable water in the samples, including the gel pore water, further measurements were made on the mortar cylinders exposed to water from one end using the laboratory GARField[RHa6].

Figure 5 shows the echo sum profile of water across the top 30 mm of a sample cured underwater for 6 months (circles). A generally uniform water distribution is observed. Also shown in Figure 5 is the profile of the same sample after oven drying at 60°C for 14 days (crosses). All the readily evaporable water is removed as evidenced by the almost total absence of signal. Water in crystalline solids and in hydrate interlayer spaces is not expected to be observed in the mortar for the echo time used. During drying, the sample lost 6.15 g of water, equivalent to 16% of the overall sample volume. This volume of water is consistent with the idea that gel and large pore water is lost, but that interlayer and water in crystalline solids remains. Based on Muller at al, the gel and large porosity in cement paste with 0.48 *w/c*, is about 40 vol% {{82 Muller,Arnaud C.A. 2013;}}. The *w/c* of the mortar was 0.5, that is very close to the 0.48 in paste as some water is usually adsorbed on the fine aggregate surface. The paste content of standard mortar is about 42 vol%, therefore the gel and large porosity in mortar is about 17 vol%. Finally, the figure shows the water profile after 24 hours of re-wetting by contact with liquid water from the sample end in a capillary uptake configuration (triangles). As evidenced by the NMR, water has completely invaded this part of the sample once more. It shows a near uniform concentration greater than that before drying. During this time the sample mass increases by only 2.13 g presumably because the sample is not wetted along the full 150 mm length. As an aside, the mass of the sample takes more than one month to stabilise and we never observed it back to the original value. This may be because a dynamic equilibrium profile is established with an evaporation front partway along the sample length or because pore-blocking prevents water penetration along the full sample length.

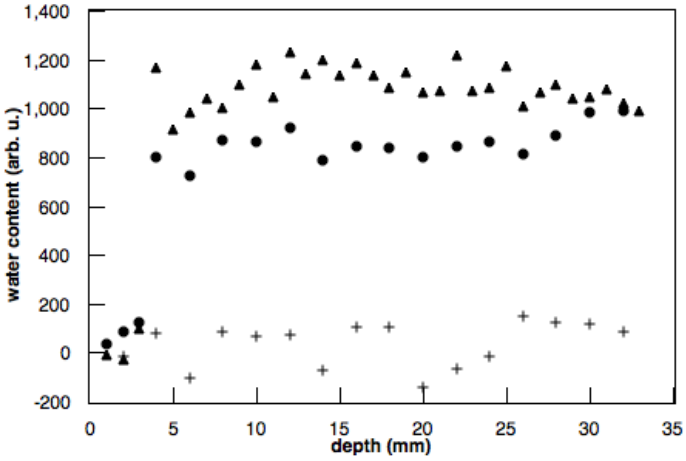

Fig 5. Profile of underwater cured sample as prepared (circles), dry (crosses) and after 1 day of capillary sorption (triangles)

The characteristic behaviour exemplified in Figure 5 was observed in most mortar samples cured both sealed and underwater. However, in a few samples, the water uptake did not pass through the full 30 mm in one day, but rather slowed dramatically, perhaps due to pore-blocking. These samples have not been included in the report of this work. In other samples cured with silica fume in the mix, the uptake was slower from the start and did not traverse 30 mm in the first day, perhaps due to a finer porosity (ref. Arnaud[N7]). These are not included.

As with the concrete, the echo sum trace does not properly reflect the whole water content by mass because the T_2 decay time is pore size dependent. The top left element of Figure 6 shows the average echo train decay in the top 11 slices (5-15 mm) of the sample before drying together with a fit to the data assuming 2 T_2 components with T_2 relaxation times of 250 and 1250 μs and a baseline. The log scale makes clear the multi-exponential character of the decay. Similar analyses of the dried sample and of the re-wetted sample after 1, 2, 4 and 7 days of rewetting are shown in the other figure elements. Notice that the scale of the dried sample is different to all the rest. There is almost no signal compared to the other traces except in the first few echoes.

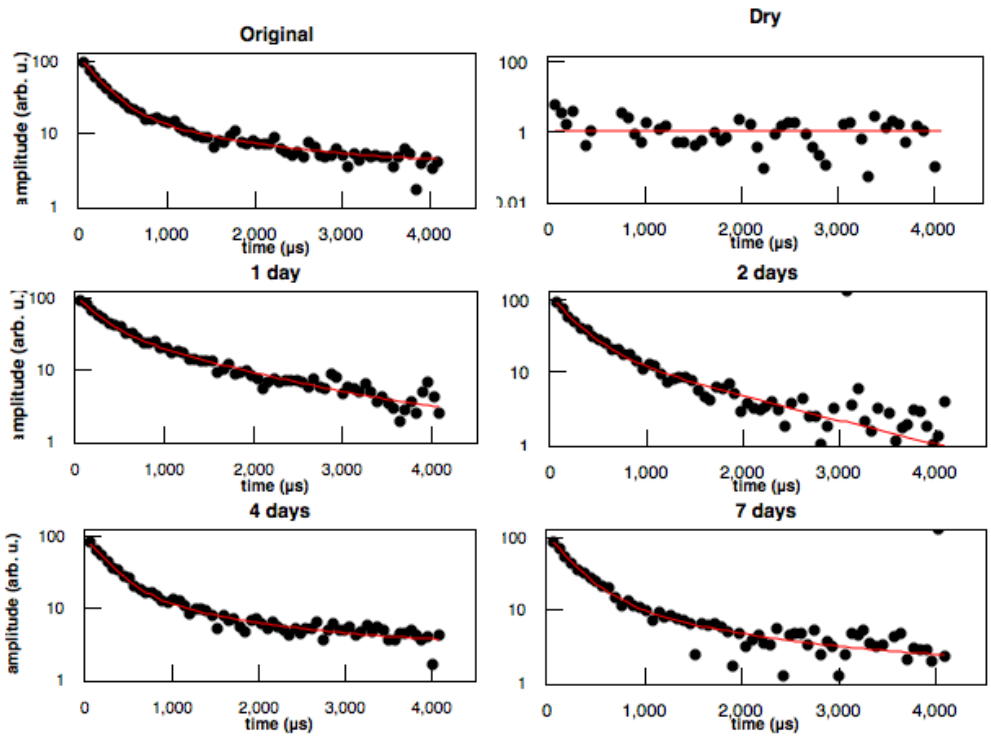

Fig 6. Average echo decay of underwater cured mortar sample at different times with 2 component fitting[N8][RHa9]

Figure 7 shows a similar echo decay and 2 component fitting (albeit for different relaxation times) for a saturated sandstone sample of the same dimensions. The data for sandstone can be directly compared to that for the mortars. The sandstone porosity is 15 % by volume as measured by pressure saturation. On this basis, the NMR signal suggests that 11 vol% of the water in the mortar has been revealed by NMR. The gel and capillary water based on mass loss upon drying suggest 16 vol%. It is possible that some of the water evaporated during drying was sheet water. However, according to Mueller et al[3]., the expected gel and capillary porosity is about 16-18 vol%.This is not consistent with laboratory GARField measurement on mortars.

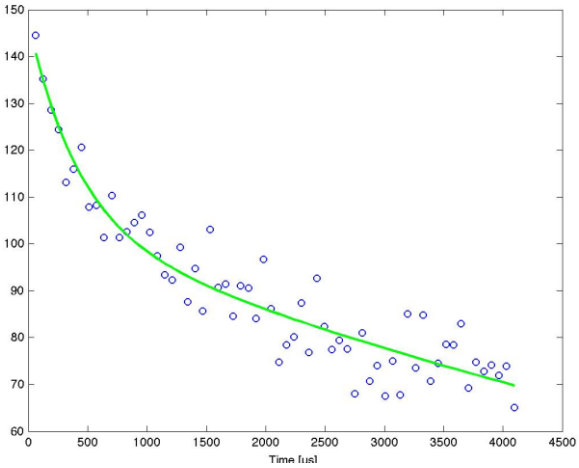

Fig 7. sandstone echo decay (not sure if this figure is really

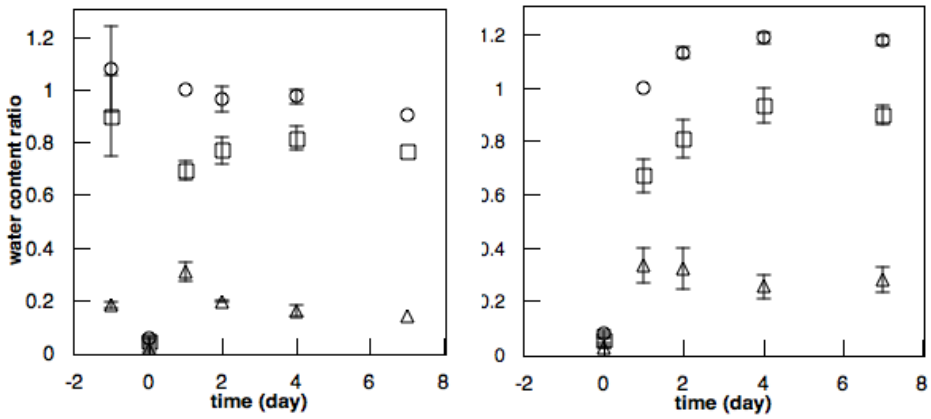

Fig 8. Water content ratio normalised to 1 day of sorption for sealed cured (left) and under water cured (right)[RHa11] samples, showing total (circles), short (squares) and long (triangles) components by time. The data at -1 day is for the as cured mortar (underwater curing only) and the data at 0 days for the dried mortars (both curing protocols). Of course, drying actually took circa 2 weeks. The data for day 1 and beyond is recorded during capillary absorption.

Figure 8 shows total average signal intensity from 5 to 15 mm of the mortar relative to that of 1 day of sorption (considered 100%) as a function of drying and re-wetting. It also shows the breakdown of the signal into the short and long components of the fit. The baseline is typically 2 % of the total, and is never more than 4 %, for mortar samples. As the baseline could be associated with a long T_2 decay, it has been added into the long component fit.

Quite noticeably, save for the dried sample (where the intensity is close to zero) the total intensity decreases slightly for the underwater cured sample whereas for the sealed cured sample it increases by about 20 %. What is also noticeable is that the total signal in the longer components after 4 days rewetting is very similar to the pre drying value, whereas at 1 day it is substantially greater. The fraction in the shorter component behaves in the opposite way. It has a minimum at 1 day. Hence, while the total signal before drying and after 1 day of rewetting are very similar, the distribution across the long and short components is very different. The long component corresponding to larger pore spaces is over represented after 1 day rewetting. After 4 days rewetting the distribution has returned to the original. In the case of the sealed cured sample, the redistribution is still there. However, now, after 1 day of rewetting, the increase in the short component exceeds the decrease in the long component leading to the increasing total. [RHa12]The experiment has been repeated for 5 mortars: 2 cured underwater and 3 cured sealed. These repeats, have been used as the basis of the error bars in Figure 8.

The absolute signal intensities in the long and short components depend critically on the choice of T_2 values used in the analysis. Hence the analysis has been repeated for different pairs of T_2 values including 250 μs and 1500 μs, and for variable T_2 within 150-450 and 1000-3000 μs ranges: although the absolute signal fractions clearly change, the story of increasing ratio of filled small pore spaces to large pore spaces remains the same.

It may be considered that the water has not fully penetrated the top 30 mm notwithstanding the evidence of Figure 5. Hence the analysis has been repeated for just the surface 5 layers. The story is the same.

The message of these experiments is that water rapidly invades large spaces in dried mortar, but that these large spaces decrease in (filled) volume with time while smaller spaces increase. The key difference between sealed and underwater cured samples, is that while the ratio of short to long signal intensity fraction increases in the days immediately following sample rewetting, the overall total of the sealed samples does in fact slightly increase with a constancy

of the long component whereas the overall total of the underwater cured samples is constant and the long component decreases.[RHa13]

Discussion

The key result seen across every sample investigated is that after initial uptake, the capillary water signal near the exposed surface decreases with time during a capillary uptake experiment. Where it has been measured, the initial uptake is to a level greater than the as-cured material. The fall-back is to the as-cured material. This observation is counter intuitive. It suggests that water first enters capillary pores then desorbs once more. In the case of the mortar samples the gel pore water is also seen. This always increases throughout the capillary uptake, sometimes, but not always attaining a constant value. In the case of the mortars, the combined gel pore and capillary total is available. It is markedly different in the cases of the sealed cured samples, where it increases throughout capillary uptake, and in the underwater cured samples where it is constant within measurement error. The curing effects how the capillary pore space is created and is possible that with fixed T_2 values show different distribution for the two curing methods.

One possibility is that the sample first fills large pores and then the smaller pores fill. However, while this could account for the more slowly increasing gel pore signal in the mortars, it seems unreasonable to expect that, in presence of a continued source of water, that they do this at the expense of the larger pores. The only reasonable explanation that we can see is that this is evidence of C-S-H gel swelling. Interhydrate porosity occuring on the length scale of 10-100 nm as described by Muller et al is lost as C-S-H swells during re-wetting, after drying. If this is the case, then the timescale of the swelling is about 1 day.

Anomalous water sorptivity have been discussed by many {{4 Hall,C. 1995; 47 Martys,Nicos S. 1997; 73 Taylor,S.C. 1999; 94 Hanžič,L. 2003; 32 Hall,Christopher 2007;}}. Two timescales were observed with gravimetry, the

water uptake significantly slowing down in case of liquid water sorptivity. This effect was not seen when organic liquids were used. ESEM micrographs suggest swelling in reaction to water.

In other measurements on pastes and mortars (Lund) [N14]have observed timescales of water uptake into macroscopic samples measured gravimetrically. It is possible that our work supports their conclusions save that we are able to look at the local water content near the surface of a large sample. The effects we see are not integrated across the whole sample, and being near the surface occur rather quickly after re-wetting starts. However, the timescale used was different to our results, most following sorptivity for the first few hours and up to 1 day, whereas the first NMR dataset was recorded after 1 day of sorption in this case.

As a final comment, we note that we have carried out further experiments on concretes made with blended cements containing silica fume or slag. These concretes show substantially the same behaviour.

Conclusions

NMR results of concrete sorptivity measurements using the Surface GARField shown that despite constant sample mass, the interhydrate and capillary water decreases after 1 day. In case of underwater cured concretes, the amount of capillary water decreased close to the original, as-cured level. As there was a constant supply of water, results suggested redistribution of water into smaller pores not visible by the equipment and taking up the largest pore spaces. Further measurements on mortars included gel water and showed that in case of underwater cured samples, additional large porosity was created during drying in expense of gel water and that after 4 days of sorption the large-small pore water was equilibrated around the original, never dried amount.[RHa15]

Acknowledgements

The research leading to these results has received funding from the European Union Seventh Framework Programme (FP7/2007-2013) under grant agreement 264448

References

I use refworks to keep track of references. References will be numbered in brackets in the text, but when I processed the document for all references, it didn't recognise the links anymore from a previous version. It's easier for the moment and just copied the references here.

[1] C. Hall, W. D. Hoff, S. C. Taylor, M. A. Wilson, B. Yoon, H. -. Reinhardt, M. Sosoro, P. Meredith and A. M. Donald. Water anomaly in capillary liquid absorption by cement-based materials. *J. Mater. Sci. Lett. 14(17),* pp. 1178-1181. 1995.

[2] S. C. Taylor, W. D. Hoff, M. A. Wilson and K. M. Green. Anomalous water transport properties of portland and blended cement-based materials. *J. Mater. Sci. Lett. 18(23),* pp. 1925-1927. 1999.

[3] A. Valori, P. J. McDonald and K. L. Scrivener. The morphology of C–S–H: Lessons from 1H nuclear magnetic resonance relaxometry. *Cem. Concr. Res. 49(0),* pp. 65-81. 2013.

[4] A. C. A. Muller, K. L. Scrivener, A. M. Gajewicz and P. J. McDonald. Densification of C-S-H measured by 1H NMR relaxometry. *J. Phys. Chem. C 117(1),* pp. 403-412. 2013.

[5] A. C. A. Muller, K. L. Scrivener, A. M. Gajewicz and P. J. McDonald. Use of bench-top NMR to measure the density, composition and desorption isotherm of C–S–H in cement paste. *Microporous and Mesoporous Materials 178(0),* pp. 99-103. 2013.

[6] S. Zamani, R. M. Kowalczyk and P. J. McDonald. The relative humidity dependence of the permeability of cement paste measured using GARField NMR profiling. *Cem. Concr. Res. 57(0),* pp. 88-94. 2014.

[7] P. S. Aptaker, P. J. McDonald and J. Mitchell. Surface GARField: A novel one-sided NMR magnet and RF probe. *Magn. Reson. Imaging 25(4),* pp. 548. 2007.

[8] P. J. McDonald, P. S. Aptaker, J. Mitchell and M. Mulheron. A unilateral NMR magnet for sub-structure analysis in the built environment: The surface GARField. *Journal of Magnetic Resonance 185(1),* pp. 1-11. 2007.

[9] P. M. Glover, P. S. Aptaker, J. R. Bowler, E. Ciampi and P. J. McDonald. A novel high-gradient permanent magnet for the profiling of planar films and coatings. *Journal of Magnetic Resonance 139(1),* pp. 90-97. 1999.

493 [10] N. C. Collier, J. H. Sharp, N. B. Milestone, J. Hill and I. H. Godfrey. The
494 influence of water removal techniques on the composition and microstructure of
495 hardened cement pastes. *Cem. Concr. Res. 38(6),* pp. 737-744. 2008.

496 [11] P. J. McDonald, V. Rodin and A. Valori. Characterisation of intra- and
497 inter-C–S–H gel pore water in white cement based on an analysis of NMR signal
498 amplitudes as a function of water content. *Cem. Concr. Res. 40(12),* pp. 1656-
499 1663. 2010.

500 [12] S. Meiboom and D. Gill. Modified spin-echo method for measuring
501 nuclear relaxation times. *Rev. Sci. Instrum. 29(8),* pp. 688-691. 1958.

502 [13] T. B. Benson and P. J. Mcdonald. Profile amplitude modulation in
503 stray-field magnetic-resonance imaging. *Journal of Magnetic Resonance, Series A*
504 *112(1),* pp. 17-23. 1995.

505 [14] M. D. Hürlimann and D. D. Griffin. Spin dynamics of Carr–Purcell–
506 Meiboom–Gill-like sequences in grossly inhomogeneous B0 and B1 fields and
507 application to NMR well logging. *Journal of Magnetic Resonance 143(1),* pp. 120-
508 135. 2000.

509 [15] N. S. Martys and C. F. Ferraris. Capillary transport in mortars and
510 concrete. *Cem. Concr. Res. 27(5),* pp. 747-760. 1997.

511 [16] L. Hanžič and R. Ilić. Relationship between liquid sorptivity and
512 capillarity in concrete. *Cem. Concr. Res. 33(9),* pp. 1385-1388. 2003.

513 [17] C. Hall. Anomalous diffusion in unsaturated flow: Fact or fiction?
514 *Cem. Concr. Res. 37(3),* pp. 378-385. 2007.

515

516

517

518